



# Direct Hybridization of Polymer Exchange Membrane Surface Fuel Cell with Small Aqueous Supercapacitors

S. Ait Hammou Taleb, D. Brown, J. Dillet, P. Guillemet, J. Mainka, O. Crosnier, C. Douard, L. Athouël, T. Brousse, O. Lottin

## ► To cite this version:

S. Ait Hammou Taleb, D. Brown, J. Dillet, P. Guillemet, J. Mainka, et al.. Direct Hybridization of Polymer Exchange Membrane Surface Fuel Cell with Small Aqueous Supercapacitors. Fuel Cells, 2018, 7th International Conference on Fundamentals & Development of Fuel Cells (FDFC 2017, 18 (3), pp.299 - 305. 10.1002/fuce.201700107 . hal-01848289

**HAL Id: hal-01848289**

**<https://hal.science/hal-01848289>**

Submitted on 19 Dec 2023

**HAL** is a multi-disciplinary open access archive for the deposit and dissemination of scientific research documents, whether they are published or not. The documents may come from teaching and research institutions in France or abroad, or from public or private research centers.

L'archive ouverte pluridisciplinaire **HAL**, est destinée au dépôt et à la diffusion de documents scientifiques de niveau recherche, publiés ou non, émanant des établissements d'enseignement et de recherche français ou étrangers, des laboratoires publics ou privés.

# Direct Hybridization of Polymer Exchange Membrane Surface Fuel Cell with Small Aqueous Supercapacitors

S. Ait Hammou Taleb<sup>1</sup>, D. Brown<sup>2,3</sup>, J. Dillet<sup>1</sup>, P. Guillemet<sup>2,3</sup>, J. Mainka<sup>1</sup>, O. Crosnier<sup>2,3</sup>, C. Douard<sup>2,3</sup>, L. Athouël<sup>2,3</sup>, T. Brousse<sup>2,3</sup>, O. Lottin<sup>1\*</sup>

<sup>1</sup>Laboratoire d'Energie et de Mécanique Théorique et Appliquée (LEMTA) UMR CNRS / Université de Lorraine 7563, Nancy, France

<sup>2</sup>Institut des Matériaux Jean Rouxel (IMN), Université de Nantes, CNRS, 2 rue de la Houssinière, BP 32229, 44322 Nantes cedex 3, France

<sup>3</sup>Réseau sur le Stockage Electrochimique de l'Energie, FR CNRS n°3459, France

## ABSTRACT

The high power density of polymer exchange membrane surface fuel cells (PEMFC) and hydrogen storage may be significantly hampered by the size and weight of the ancillaries needed to control air and hydrogen flow rates and humidity. In order to overcome these difficulties, a variety of research has been carried out on the development of hybrid systems based on supercapacitors or batteries, which raises questions about the best architectures and control strategies and may, if not well mastered, enhance the complexity of the entire system. In this study, we focus on the direct hybridization of PEMFC and supercapacitors (SCs) - using one unit per cell - with the ultimate objective of inserting flat aqueous carbon/carbon SCs within a fuel cell stack. This first experimental work shows that a minimum capacity of about  $1 \text{ F.cm}^{-2}$  (with reference to the PEMFC active surface) and a maximum series resistance of about  $0.5 \Omega.\text{cm}^2$  are sufficient to back up the cell during load variations such as a sudden increase in the current density: this makes it possible to always supply the fuel cell with the right amount of gas without anticipating current peaks or load transients. Flat supercapacitors were also designed, manufactured and tested during this project; they performed better than commercially available cylindrical supercapacitors of identical capacity because of a lower series resistance.

**Keywords:** Fuel cell, supercapacitors, direct hybridization, PEMFC, stack, load transients.

## 1. Introduction

PEMFC can produce electricity as long as they are fed with oxygen and hydrogen: that is the reason why their energy density can approach that of hydrogen storage systems in the case of the most powerful systems. However, their high power density may be significantly hampered by the size and weight of the ancillaries needed to control air and hydrogen flow rates and humidity [1, 2]. On top of that, fuel cell dynamics (i.e. their ability to respond to a sudden increase in power demand) may also be limited by the gas supply lines: compressor, flow controllers and/or humidifiers. Indeed, due to

---

\* Corresponding author : Olivier.Lottin@univ-lorraine.fr

usual requirements in terms of electric efficiency and compactness, Gas Diffusion Layers (GDL) that are used to homogenize the gas flow to the reaction sites and conduct the electrons [3 ,4], as well as the flow field channels, can store only a very limited amount of reactants. Thus, an increase in current intensity and electrical power must be accompanied by an immediate increase of the hydrogen and air/oxygen flow rates, which can be difficult to achieve.

In order to overcome these difficulties, a variety of research has been carried out on the development of hybrid systems based on batteries or supercapacitors [5, 6]. Unlike PEMFC, supercapacitors (SCs) are able to supply high power (with reference to their weight) but cannot store an important amount of energy (Figure 1). In these regards, fuel cells and supercapacitors (also called electrochemical capacitors) can be considered as complementary.

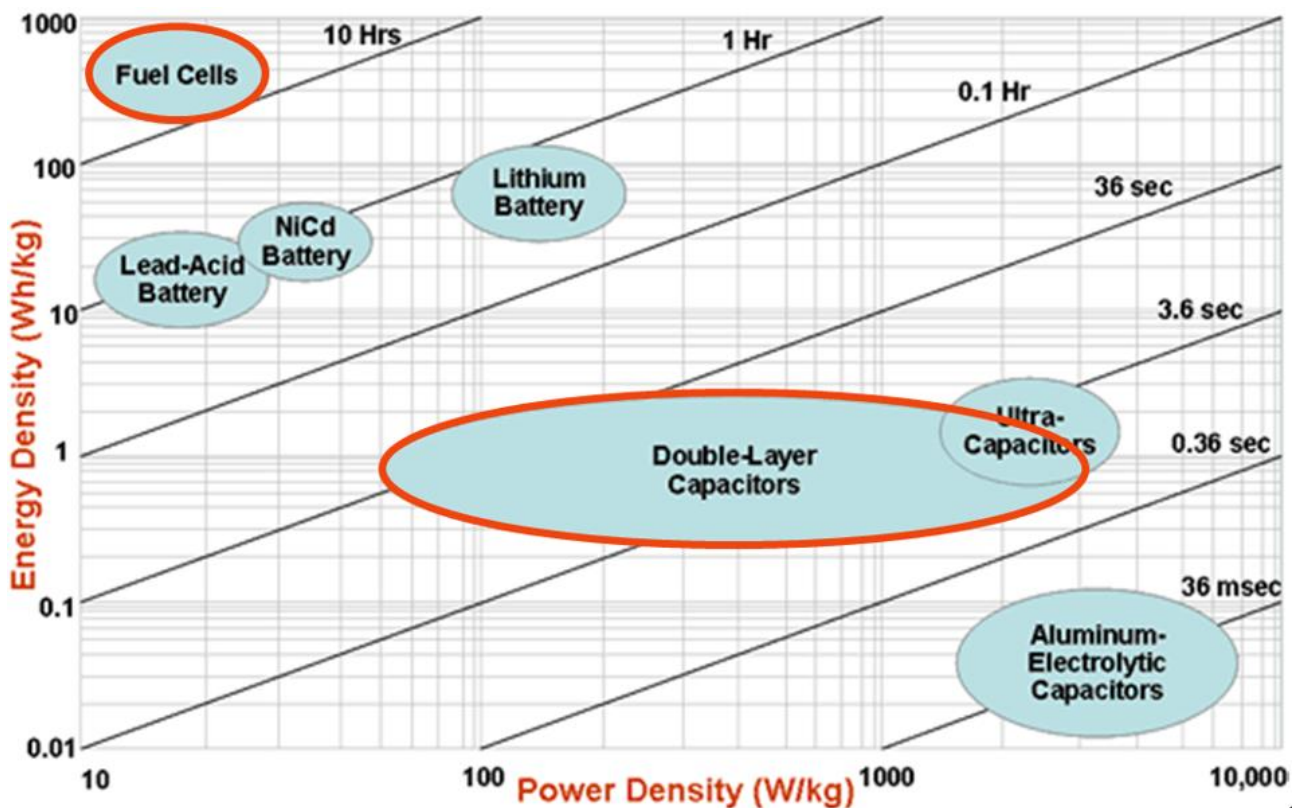


Figure 1 : Ragone plot of various energy devices and their charge times (diagonal strokes) [7].

However, if hybridization with supercapacitors can improve the performance of fuel cell systems, questions remain about the best architectures and control strategies. The complexity and cost of the entire system must remain reasonable and hybridization must not be done at the expense of the fuel cell durability and reliability.

Currently, most of hybrid fuel cell/supercapacitor systems include power management units [8] with two possible designs depending on whether one or two DC/DC converters are used:

- Two converters, one for the fuel cell and the other for the supercapacitor bank, make it possible to control independently the power provided by each source...
- ... but only one DC/DC converter connected to the fuel cell can be enough to maintain the fuel cell voltage in a given range.

Nevertheless, power management units and DC/DC converters can be avoided by using direct (or passive) hybridization, i.e. by connecting directly the supercapacitors to the cells. In this case, there also exist two possible configurations:

- One SC can be connected to two cells in series [9], which is possible because commercial SCs with organic electrolytes can accept voltages up to 2.7 V.
- Each SC can be connected to an individual cell, which is the choice we have made. This makes it possible to use SCs with aqueous electrolytes since the cell voltage always remains below 1 V. However, in this case, the SC will be subjected to small potential variations, i.e. of the order of a few hundredth of *mV*.

In this work, we study the effect of passive hybridization to improve the system performance and reliability, more specifically during steep load variations. We show that during the short time needed by the gas supply lines to respond to an increase in power or current density, SC of about  $1\text{ F.cm}^{-2}$  (with reference to the MEA flat area) are required to limit the system voltage drop to acceptable values.

## 2. Experimental set-up

### 2.1 Fuel cell

All experimental results described in the following were obtained using a  $98\text{ mm} \times 20\text{ mm} = 19.6\text{ cm}^2$  cell active area with eleven  $1\text{ mm} \times 99\text{ mm}$  parallel channels of 0.4 mm in depth on both the anode and cathode side. Membrane-Electrode Assemblies (MEAs) were purchased from SolviCore GmbH & Co. KG under the commercial name H400E. We assumed a cathode Pt loading of about  $0.4\text{ mg}_{\text{Pt}}.\text{cm}^{-2}$ , the exact value being not given by the manufacturer. On both anode and cathode sides, the gas diffusion layers (GDL) coated with microporous layer (MPL) were  $235\text{ }\mu\text{m}$  thick SGL 24BC (by SGL Carbon) compressed to  $200\text{ }\mu\text{m}$  using Teflon gaskets. Both gases flew in the same (vertical) direction. The cathode compartment was supplied with wet air (70% RH at FC operation temperature and a stoichiometry of 3). Unless otherwise stated, the fuel cell was operated with a dead-ended anode: i.e. the anode outlet was closed except during 1 s every 60 s to flush the compartment. Hydrogen was not humidified and a pressure regulator kept its pressure to 1.3 bar. In section 4.2, we also present results

obtained with an open anode: in this case, the hydrogen stoichiometry was set to 1.2 and it was humidified to 70% *RH* (at FC operation temperature).

The FC temperature was kept to 60°C thanks to an external thermostated cooling circuit.

Each new MEA was subjected to a 2 hours conditioning stage consisting of 45 s current steps between open circuit, 0.4 A.cm<sup>-2</sup> and 1 A.cm<sup>-2</sup>.

## 2.2 Small aqueous supercapacitors

### Basics characteristics of SCs

The two principle characteristics of a SC are its high frequency or series resistance  $R$  and its (equivalent) capacity  $C$ . As illustrated in Figure 2, the simplest SC equivalent circuit consists in setting these two components in series. The response time of the system is then  $\tau = R \times C$ .

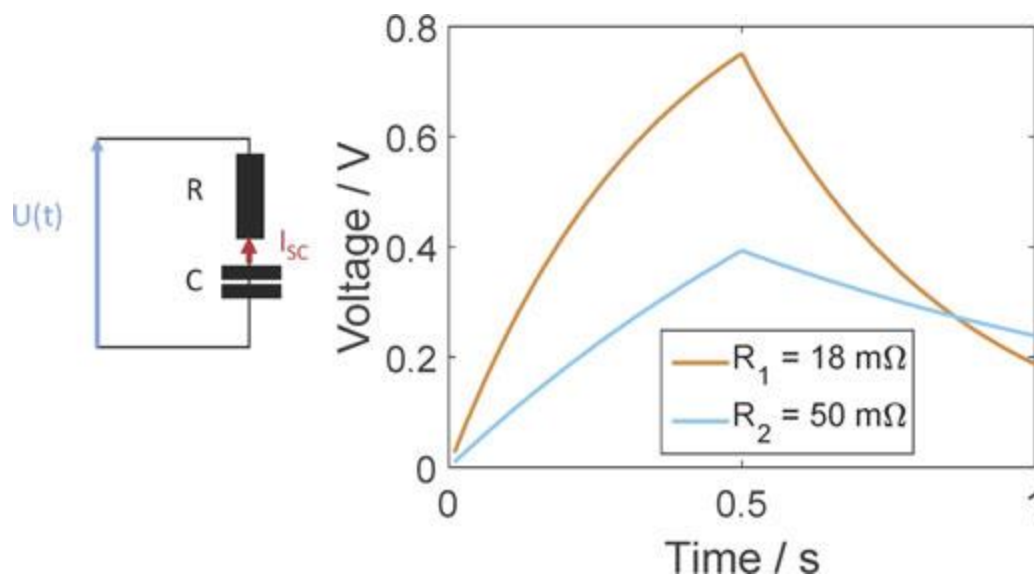


**Figure 2: Simplest SC equivalent circuit (left) and the corresponding charge and discharge of a RC circuit (right) with different values of series resistance and identical capacity during 0.5 s current steps of  $\pm 1 \text{ A}$ .**

Figure 2 shows the voltage vs. time charge and discharge curves of two SCs with different resistance values and identical capacities for a 0.5 s current step of  $\pm 1 \text{ A}$ . The resistance of circuit 1 (in blue) is four times lower than that of circuit 2 (in red). As can be seen, a higher resistance increases the SC characteristic time, that is to say the charge or discharge time. This clearly shows that in the case of hybridization with a FC, the performance of a SC does not only depend on its capacity but also on its high frequency (or series) resistance.

## Use of flat supercapacitors

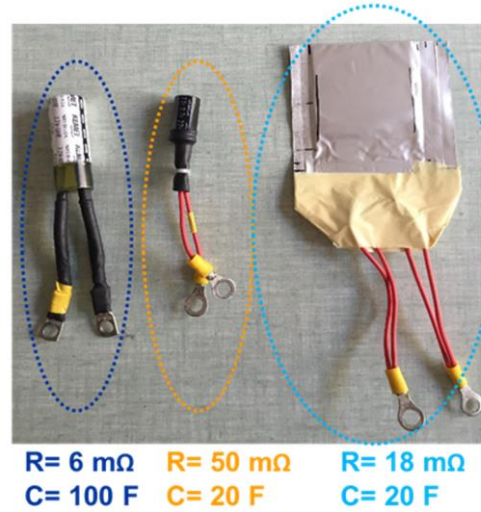


**Figure 3: Commercial (organic) and flat aqueous SC. The latter were designed and assembled during the project. Values of R and C were identified starting from charging curve (time response) at  $I = 1 \text{ A}$  between  $0 \text{ V}$  and  $1 \text{ V}$  with uncertainties of about  $5 \text{ F}$ ,  $1 \text{ m}\Omega$  for the  $100 \text{ F}$  commercial SC and  $1 \text{ F}$ ,  $2 \text{ m}\Omega$  for the two others.**

Flat aqueous supercapacitors were also designed and manufactured in the framework of this project: indeed, low maximum voltages of about one volt per cell and a temperature limited to about  $80^\circ\text{C}$  allow to use alternative and safe materials such as activated carbon electrodes in PVDF binder (10%), and  $5\text{M LiNO}_3$  as electrolyte instead of organic liquids. In order to lower the high frequency resistance as much as possible, the electrodes were set on gold plated nickel collectors. Details about manufacturing techniques and materials are out of the scope of this paper and will be published shortly. We associated SCs of about  $20 \text{ F}$  to  $19.6 \text{ cm}^2$  fuel cells, i.e.  $1 \text{ F.cm}^{-2}_{\text{MEA}}$ , which is relatively low compared to the hybrid systems usually encountered in the literature, but the performance remains satisfying due to a very good high frequency resistance of only  $18 \text{ m}\Omega$  (compared to about  $50 \text{ m}\Omega$  for equivalent commercial products, Figure 3). The  $100 \text{ F}$  commercial SC appearing in Figure 3 was used for comparison purpose -for the hybridization of a single cell-, as well for the hybridization of a small stack described in section 5.

One of the objectives of this project is to reduce the size of the system by using flat SCs that will be set close to the FC stack or even inserted between two adjacent cells inside the stack.

### 3. PEMFC behavior during steep load variations

During steep load variations such as Heaviside steps, gas flow rates cannot be adjusted rapidly enough to maintain proper hydrogen and air supplies to the cell because of the limited dynamics of the air compressor, air or hydrogen mass flow controllers or even gas humidifiers. That is the reason why when significant load variations are expected, gas stoichiometries are usually set to values higher

than required. As a result, the fuel cell operates frequently in non-optimal conditions, energy is lost due to unnecessarily high consumption of the ancillaries, and many of the system components are oversized, which impacts its cost and energy weight density.

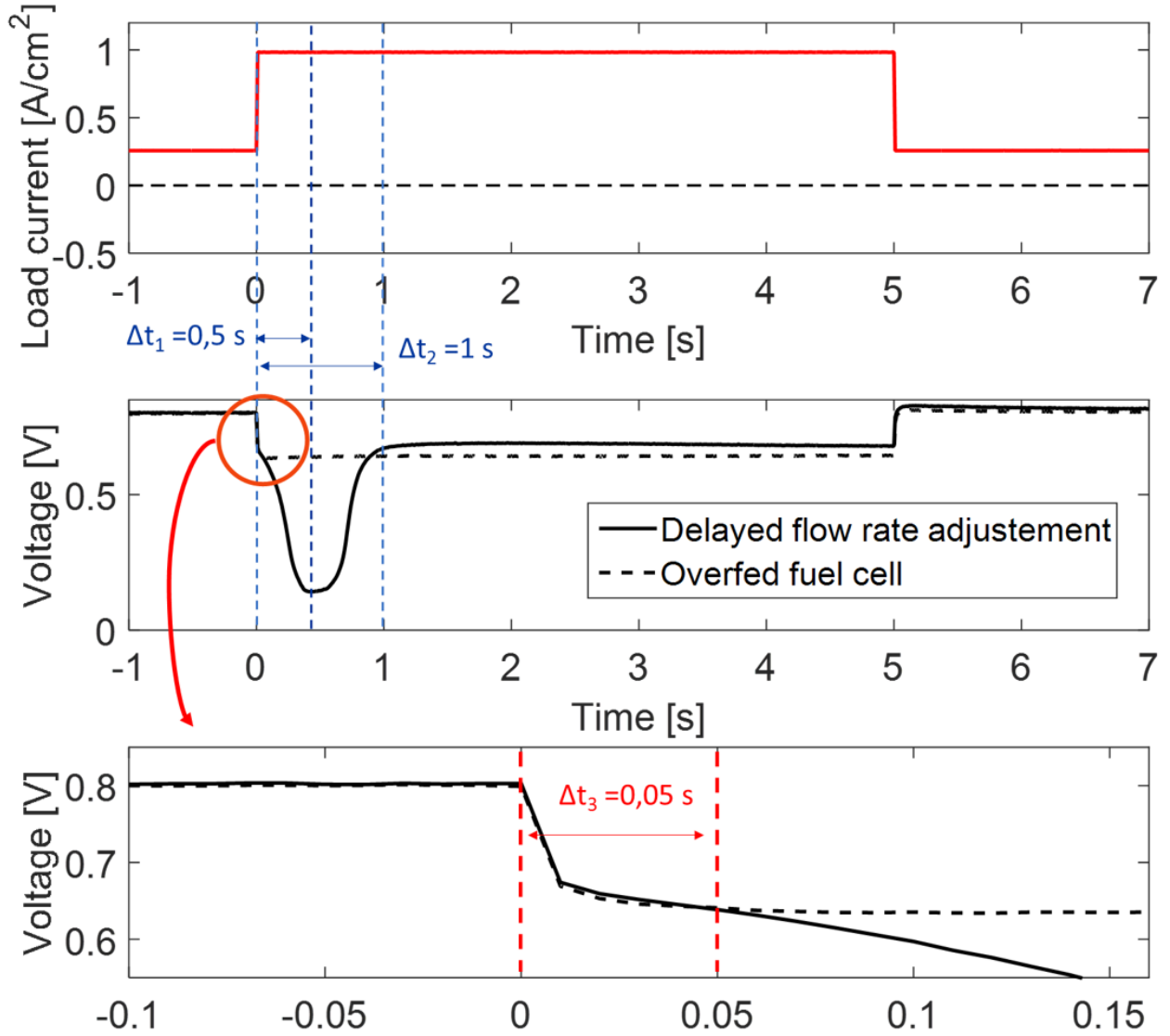


Figure 4: Fuel cell voltage during a current step of 5 s from 0.25 A.cm<sup>-2</sup> to 0.95 A.cm<sup>-2</sup>.

Figure 4 shows the cell voltage evolution during a 5 s current step from 0.25 to 0.95 A.cm<sup>-2</sup>. Flow rate inputs were changed accordingly at  $t = 0$  s and  $t = 5$  s. During half a second, the voltage decreased because of the lack of oxygen (and possibly hydrogen) in the cathode and anode compartments because the mass flow controllers failed to adjust rapidly enough the flow rates. The voltage came back to its nominal value after about 1 s when the fuel cell was fed again with the right amount of gas (i.e. when the mass flow controllers delivered the appropriate flow rate). To validate this explanation of the initial FC voltage drop, the second graph in Figure 4 shows a comparison with the voltage evolution of an overfed fuel cell (i.e. the air and hydrogen flow rates were adjusted to a



current density of  $0.95 \text{ A.cm}^{-2}$  before the  $5 \text{ s}$  increase of the current intensity). As shown in Figure 4, right at the beginning of the step, the voltage is identical (or very close) in both cases and the voltage of the underfed fuel cell (full line in Figure 4) dropped further only after  $0.05 \text{ s}$ , while that of the – initially- overfed cell remained constant during the whole sequence (dashed line in Figure 4).

These results show that our FC has a “survival time” of about  $0.05 \text{ s}$  to a Heaviside step current variation from  $0.25$  to  $0.95 \text{ A.cm}^{-2}$ , which corresponds to the time needed to deplete significantly  $\text{O}_2$  and/or  $\text{H}_2$  in the cathode and/or anode compartments. This “survival time” is much lower than the response time needed by the mass flow controllers (and gas lines) to provide the FC with the right amount of reactants. The objective of FC/SC hybridization is thus to allow the system to properly operate during these  $0.5 \text{ s}$ , the fuel cell remaining the main electric source the rest of the time.

As shown in the next section, a SC of only  $20 \text{ F}$  and  $18 \text{ m}\Omega$  series resistance connected to our  $19.6 \text{ cm}^2$  cell is able to release about  $60\%$  of its stored energy during  $0.5 \text{ s}$ , which considerably limits the fuel cell voltage drop.

## 4. Direct hybridization of a single PEMFC with a supercapacitor

### 4.1 Comparison between flat and commercial supercapacitors and impact of fuel cell cathode operating conditions

Figure 5 shows the FC voltage as well as FC and SC current time-evolutions during a total current (i.e. the sum of the SC and FC currents) step of  $5 \text{ s}$  from  $0.25 \text{ A.cm}^{-2}$  to  $0.95 \text{ A.cm}^{-2}$ . The  $19.6 \text{ cm}^2$  fuel cell was connected in parallel either with the flat aqueous ( $20 \text{ F} - 18 \text{ m}\Omega$ , blue curves) or a commercial SC ( $20 \text{ F} - 50 \text{ m}\Omega$ , orange curves). The data recorded with the FC alone appears in grey.

As expected, hybridization limits the voltage drop and the results were better with the flat  $20 \text{ F} - 18 \text{ m}\Omega$  SC than with the commercial  $20 \text{ F} - 50 \text{ m}\Omega$  SC: this is mostly due to the lower high frequency resistance of the flat SC (§ 2.2), which makes it possible to deliver more current at the beginning of the sequence. This better performance of the SC with a lower resistance remained valid whatever the step duration, i.e. from  $0.1$  to  $10 \text{ s}$  in our case, as illustrated in Figure 6.



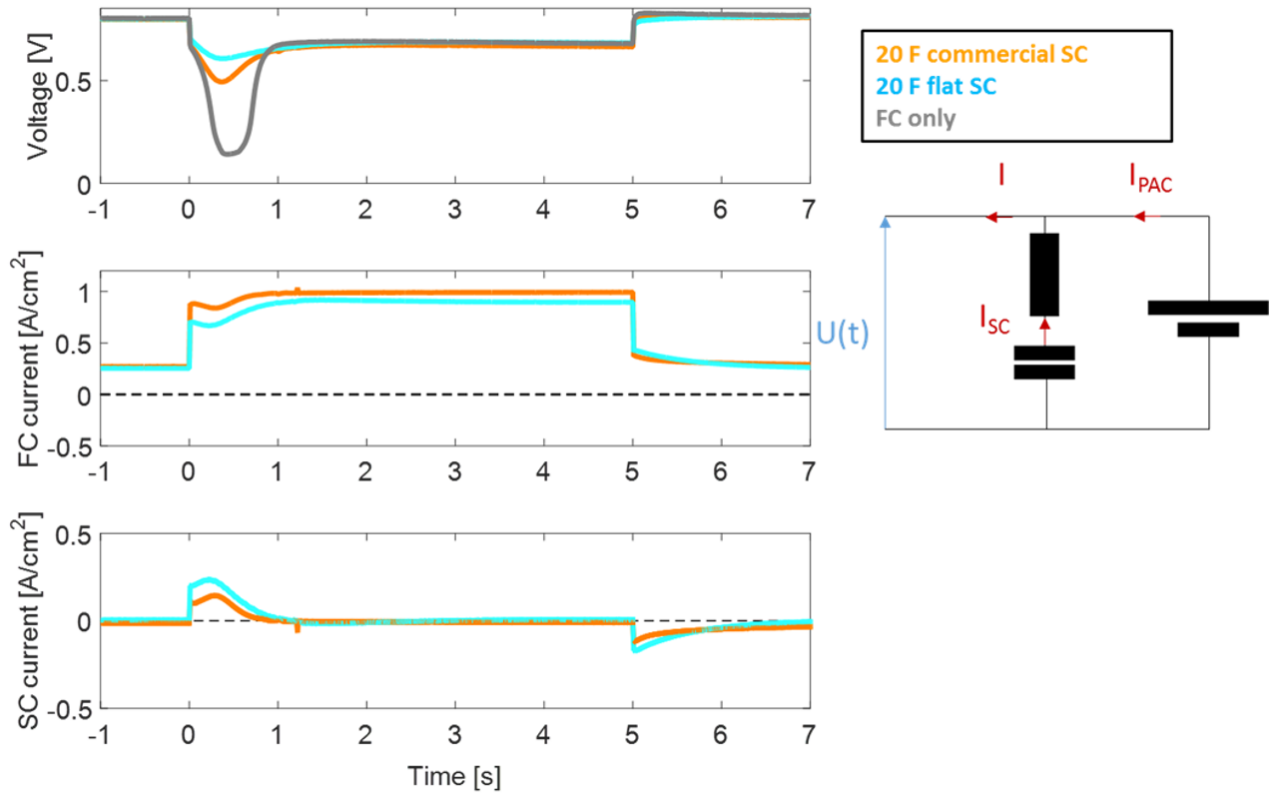


Figure 5: System voltage as well as FC and SC currents vs. time during a 5 s load step from  $0.25 \text{ A.cm}^{-2}$  to  $0.95 \text{ A.cm}^{-2}$ . The capacitance and resistance set in parallel to the single cell stand for the SC equivalent circuit.

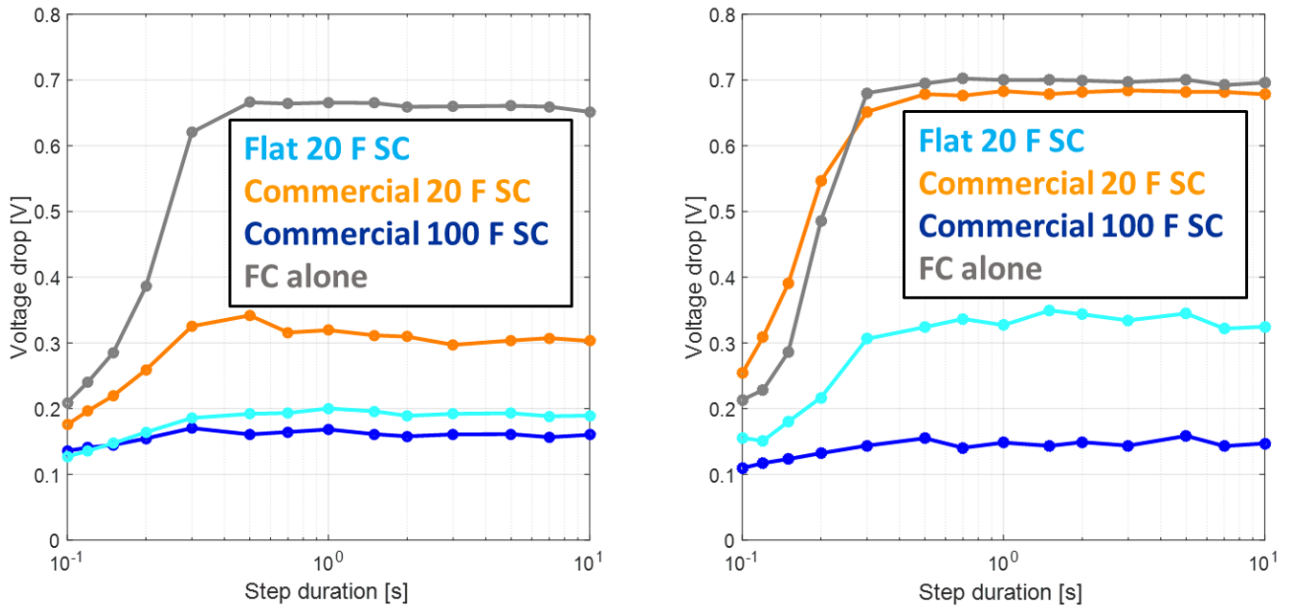
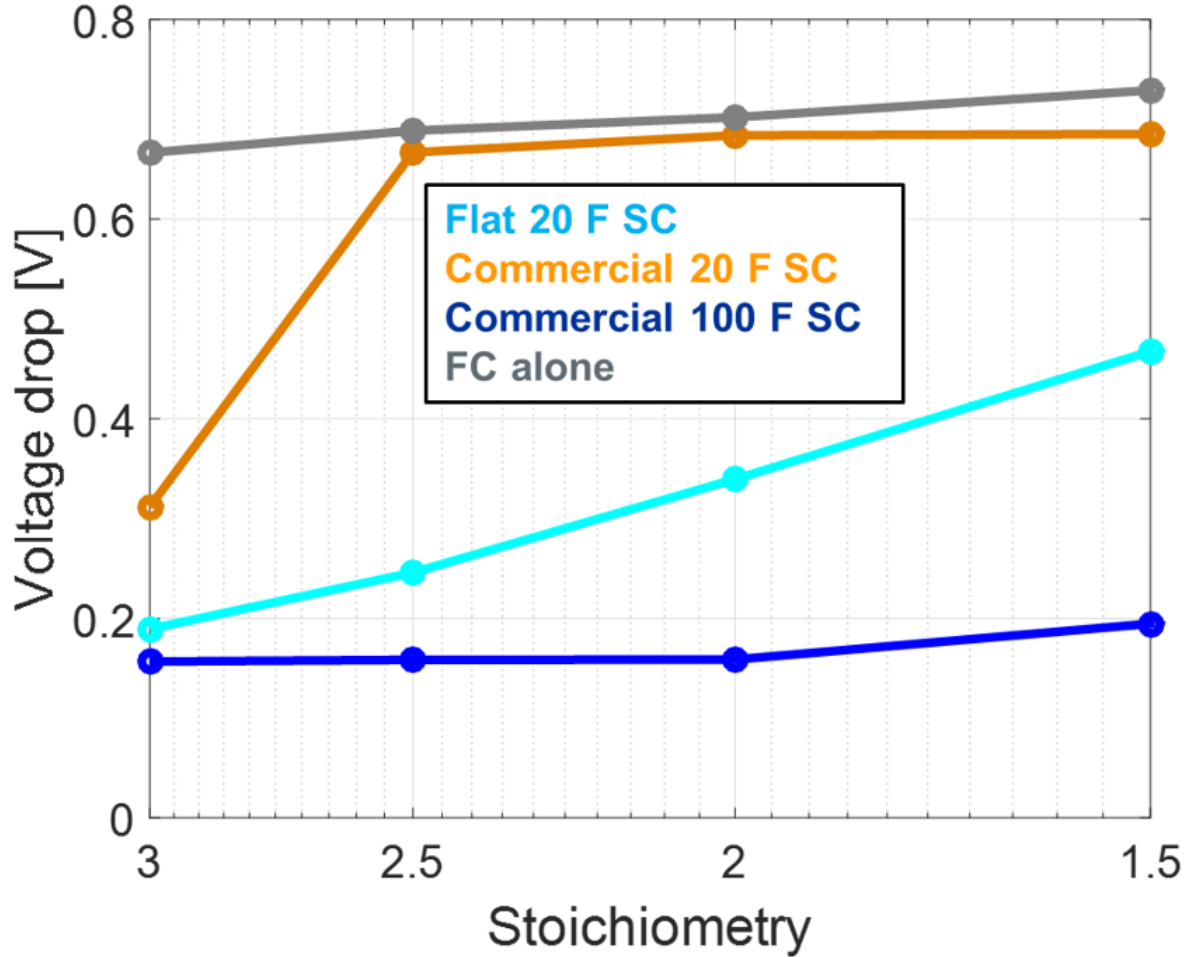


Figure 6: Left, voltage drop vs. load step duration, air stoichiometry of 3 and right, the voltage drop vs. load step duration, air stoichiometry of 2, current intensity increased from  $0.25$  to  $0.5 \text{ A.cm}^{-2}$ . On the right graph, the maximum drop obtained with the FC alone corresponds to a FC voltage of about  $0 \text{ V}$  starting from an initial value of  $0.7 \text{ V}$ .

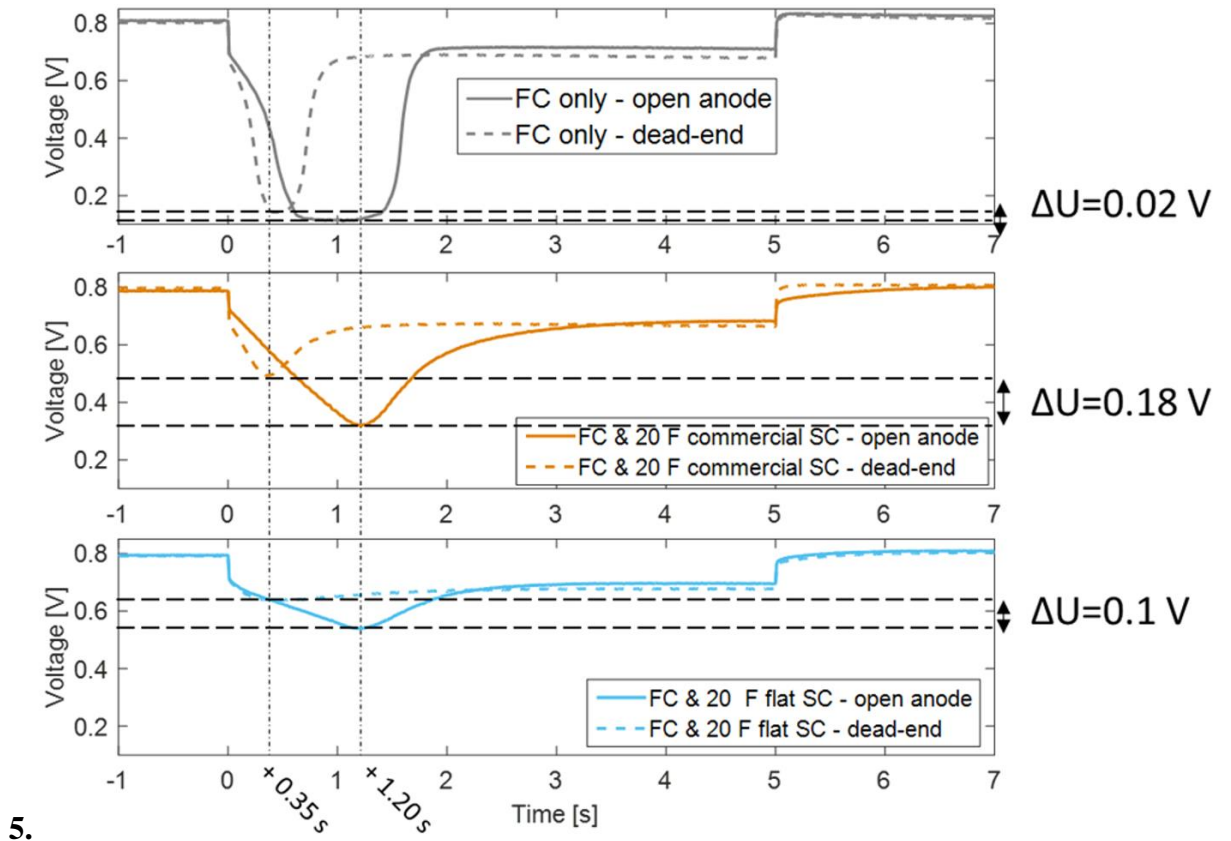
Furthermore, it comes out that the performance of the flat SC ( $20\text{ F} - 18\text{ m}\Omega$ ) is close to that of a commercial SC of  $100\text{ F}$  and  $6\text{ m}\Omega$  (Figures 6, left graph). When the air stoichiometry was lowered to 2, the hybridization with the ( $20\text{ F} - 50\text{ m}\Omega$ ) commercial SC became inefficient (see the orange curve in Figure 6, right graph) while satisfying results were still obtained with our flat  $20\text{ F}$  SC. In this case however, the commercial  $100\text{ F}$  SC performed significantly better.



**Figure 7: Maximum voltage drop vs. air stoichiometry for an increase of the current intensity from 0.25 to  $0.5\text{ A}\cdot\text{cm}^{-2}$ .**

Figure 7 shows with more detail the effect of air stoichiometry on the maximum voltage drop during a current step of more than  $1\text{ s}$  (which is the time needed to reach the lowest voltage value). This confirms that the system performance remains much more satisfying with the flat  $20\text{ F}$  ( $18\text{ m}\Omega$ ) SC than with the commercial  $20\text{ F}$  ( $50\text{ m}\Omega$ ) SC because of its lower high frequency resistance. Using the  $100\text{ F}$  ( $6\text{ m}\Omega$ ) commercial SC significantly improved the performance of the hybrid system only for air stoichiometries lower than 2.

## 4.2 Impact of fuel cell anode operating conditions



5.

6. **Figure 8: Voltage time-evolution during Fuel Cell operation with dead-ended or open anode, with and without hybridization using 20F SCs with different series resistances (50 mΩ with the commercial SC and 18 mΩ with the flat SC).**

Figure 8 shows the cell voltage evolution during the 5 s current step (still from  $0.25$  to  $0.95 \text{ A.cm}^{-2}$ ), with and without hybridization for different anode operating conditions: open anode (full lines) and dead-end mode (dashed lines); the operating conditions are described in section 2.1 for both cases. The current density and flow rate inputs were changed simultaneously at  $t = 0 \text{ s}$ . In this section, we discuss the response time of the whole system (i.e. mass flow controller(s), humidifiers, pipes and fuel cell) depending on the anode operating conditions. The impact of hybridization is analyzed using commercial (organic) and our flat (aqueous) SC of same capacity (20 F) but different series resistance ( $50 \text{ m}\Omega$  and  $18 \text{ m}\Omega$ ).

The first graph of Figure 8 shows the voltage evolution of the fuel cell alone (i.e. without hybridization). With an open anode (full grey line) the voltage decreased because of the lack of oxygen and hydrogen in the cathode and anode compartments and started to increase again only after  $1.2 \text{ s}$ . It came back to its nominal value after about  $2 \text{ s}$  when the fuel cell was fed again with the proper amount of gas. With a dead-ended anode however (dashed grey line) the system dynamics were better,

the full sequence (voltage drop and recovery) lasting only about 1 s, i.e. half as long as with an open anode. The voltage drop was also slightly less pronounced than with an open anode with a difference of 0.02 V.

Interestingly, this improvement in the system dynamics when shifting from open to dead-ended anode occurred with the same magnitude when the fuel was connected to either the 20 F commercial SC or to our lab-designed 20 F flat SC (middle and bottom graphs in Figure 8): in any case, the voltage recovery started after 0.35 s vs. 1.2 s initially, which is more than three times shorter. On top of that, the voltage drop was always less significant with a dead-ended anode, with a difference ranging from 0.1 V (flat Sc) to 0.18 V (commercial SC).

Discussing the details of the physical phenomena entailing such a change in behavior would be out of the scope of the paper. However, there are a few points that may be worth underlining:

- Although the cathode is (rightfully) considered as the limiting electrode, the transients of a PEM fuel cell are also governed by the anode. Indeed, the hydrogen stoichiometry being usually much lower than that of air, any increase in the current intensity will result in significant hydrogen starvation in the anode compartment.
- Such hydrogen starvation events must be considered with care because they can impact the cell durability and reliability. Indeed, many works showed that hydrogen starvation resulted in dramatic local (or even global) anode and cathode potentials surges, along with severe damages to the cathode materials [10 - 15].
- In our case, operating the fuel cell with a dead-ended anode always resulted in a better response to an increase in the current intensity than with an open anode, which is probably due to the combining effects of a higher hydrogen pressure (1.3 bar vs. atmospheric pressure with the open anode) and a shorter response time of the pressure regulator than that of the hydrogen mass flow controller.
- Nevertheless, it must be kept in mind that in dead-end mode the hydrogen content in the anode compartment may vary significantly, locally and with time, depending on the moment the last opening of the anode outlet occurred. In our case, the anode outlet was opened for 1 s every 60 s in order to flush entirely the anode compartment, thus preventing local hydrogen starvation. However, without a careful monitoring of the anode local potentials, we cannot affirm that such events did not occur.
- Finally, the three graphs in Figure 8 show that connecting directly a SC in parallel does not modify the dynamics of the FC/ancillary system but only limits or avoids excessive voltage drops following an increase in the current intensity.

## 7. Direct hybridization of a small stack

Direct hybridization allows connecting one SC per cell, which can be particularly interesting regarding the non-homogenous operating conditions along a stack, especially during transients. The mini-stack used for the present study was made of 3 cells (Figure 9). Cell #1 is close to the hydrogen inlet while cell #3 is close to the air inlet. Both gases flew in the same direction (i.e. in co-flow) within the cells, from the top to the bottom. Each cell was connected individually to a ( $100\text{ F} - 6\text{ m}\Omega$ ) commercial SC (see Figure 3) and in the example described below, the stack was subjected to the 5 s current step from  $0.25\text{ A.cm}^{-2}$  to  $0.95\text{ A.cm}^{-2}$  (Figure 4). As described above in the case of single cells, the air flow rate input was changed with the current density, at the beginning and at the end of the sequence. However, when operating a stack the air flow controller needed about 1 s to adapt to the new value. The hydrogen compartment was operated in dead-end mode (dry  $\text{H}_2$ ,  $P_{\text{H}_2} = 1.3\text{ bar}$ , anode compartment bled every 60 s during 1 s). As shown in Figure 9 (bottom right), without SC hybridization the stack voltage decreased dramatically during the first second following the current step and the voltage of the individual cells evolved differently. Conversely, when the cells were connected to the SCs, the stack and cell voltage behave as if there was no gas shortage (bottom left in Figure 9). Note furthermore that SC hybridization results in identical or at least very similar voltage evolution of the individual cells.

Although the stack performance and architecture may be improved, the results in Figure 9 clearly show that direct hybridization of each cell with a small SC can significantly improve the reliability and performance of a stack during transients.

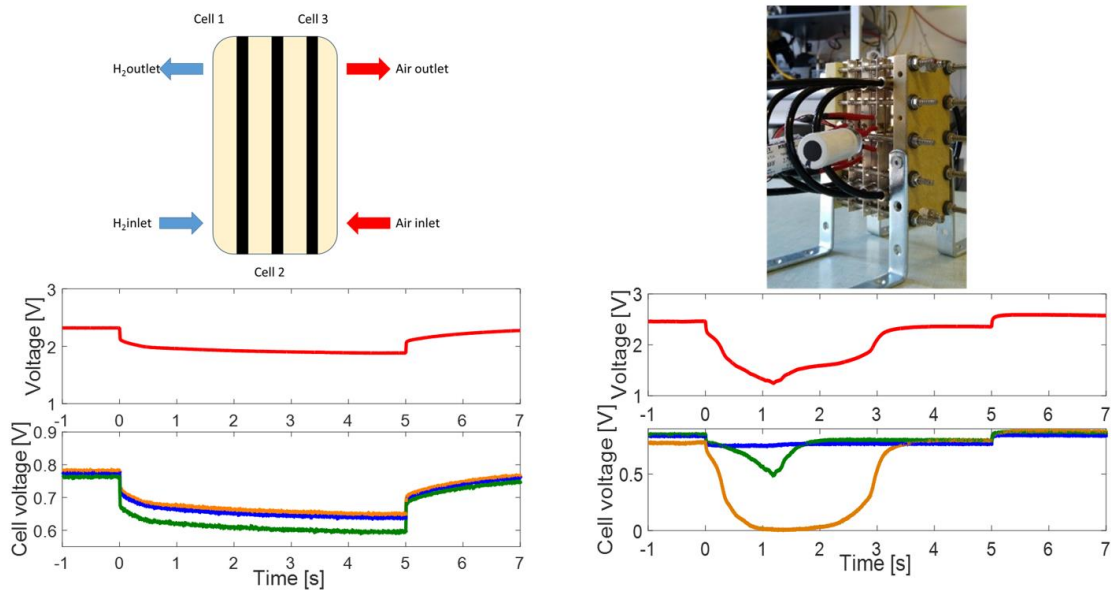


**Figure 9:** Scheme of our 3 cells stack (top left) and picture (top right). Cell dynamics in a small stack with (bottom left) and without (bottom right) hybridization of each cell (with a 100 F commercial SC) during a 5s current step from  $0.25\text{ A.cm}^{-2}$  to  $0.95\text{ A.cm}^{-2}$  (Figure 4).

## 8. Conclusion

The present work shows that direct hybridization of a PEMFC with small aqueous SC opens perspectives to more efficient, simpler and more reliable FC systems. Indeed, passive hybridization makes it possible to avoid additional electronic components such as inverter(s), not to oversize the mass flow controllers and/or air compressor and eventually to reduce the cost and weight of the system. Furthermore, connecting all cells of a stack individually to a SC may be a convenient way to homogenize their voltage evolution during transients. Such kind of hybrid architecture can be achieved using small SCs of low effective capacity but it is of primary importance to keep their high frequency resistance as low as possible to improve their response time. We also noticed that the system dynamics was better when the anode compartment was operated in dead-end mode (with a  $1\text{ s}$  opening every  $60\text{ s}$ ) than with an open outlet. Using a dead-ended anode can lead to further system simplifications: a pressure regulator can be used instead of a mass flow controller for instance and hydrogen humidifier or recycling loop are not needed anymore.

### Acknowledgements:

The authors would like to thanks French DGA/ANR for financial support of SUPERCAPAC project within the framework of ASTRID program.

## 9. References:

1. Yan, Q., H. Toghiani, and H. Causey, *Steady state and dynamic performance of proton exchange membrane fuel cells (PEMFCs) under various operating conditions and load changes*, Journal of Power Sources, **2006**, pp. 492-502.
2. Kim, S., S. Shimpalee, and J.W. Van Zee, *The effect of stoichiometry on dynamic behavior of a proton exchange membrane fuel cell (PEMFC) during load change*. Journal of Power Sources, **2004**, pp. 110-121.
3. Larminie, J. and A. Dicks, *Fuel Cell Systems Explained*, WILEY, **2003**, pp. 67 - 118.
4. N.Mugerwa, L.J.M.B.A.M., *Fuel cell systems*, KA/PP, **1993**, pp. 19 - 69
5. Azib, T., et al., *An Innovative Control Strategy of a Single Converter for Hybrid Fuel Cell/Supercapacitor Power Source*. Industrial Electronics, IEEE Transactions on, **2010** pp. 4024-4031.
6. Thounthong, P., et al., *Analysis of Supercapacitor as Second Source Based on Fuel Cell Power Generation*. Energy Conversion, IEEE Transactions on, **2009**, pp. 247-255.
7. Scott J. Moura, J.B.S., Donald J. Siegel, Hosam K. Fathy, Anna G. Stefanopoulou, *Education on Vehicle Electrification: Battery Systems, Fuel Cells, and Hydrogen*, IEEE Vehicle Power and Propulsion Conference, **2010**, pp. 1 - 6.
8. Azib, T., et al., *Système hybride à pile à combustible et supercondensateur : Structures, contrôle-commande et gestion d'énergie*. European Journal of Electrical Engineering, **2011**, pp. 363-382.
9. Morin, B., *Ph.D. Thesis*, Institut National Polytechnique de Toulouse - INPT, France, **2013**.
10. S. Abbou, J. Dillet, G. Maranzana, S. Didierjean, O. LOTTIN, *Local potential evolutions during proton exchange membrane fuel cell operation with dead-ended anode – Part I: Impact of water diffusion and nitrogen crossover*, Journal of Power Sources, **2017**, pp. 337-346,.
11. S. Abbou, J. Dillet, G. Maranzana, S. Didierjean, O. Lottin, *Local potential evolutions during proton exchange membrane fuel cell operation with dead-ended anode – Part II: Aging mitigation strategies based on water management and nitrogen crossover*, Journal of Power Sources, **2017**, pp. 419-427.
12. Borup et al., *Scientific aspects of polymer electrolyte fuel cell durability and degradation*, Chem. Rev., **2007**, pp. 3904-3951
13. Spornjak et al., *Influence of the microporous layer on carbon corrosion in the catalyst layer of a polymer electrolyte membrane fuel cell*, J. Power Sources, **2012**, pp. 386-398
14. J. Durst, A. Lamibrac, F. Charlot, J. Dillet, L. F. Castanheira, G. Maranzana, L. Dubau, F. Maillard, M. Chatenet, O. Lottin, *Degradation heterogeneities induced by repetitive start/stop events in Proton Exchange Membrane Fuel Cell: Inlet vs. Outlet and Channel vs. Land*, Applied Catalysis B: Environmental, **2013**, pp. 416-426.
15. O. Lottin, J. Dillet, G. Maranzana, S. Abbou, S. Didierjean, A. Lamibrac, R.-L. Borup, R. Mukundan, D. Spornjak, *Experimental Results with Fuel Cell Start-up and Shut-down. Impact of Type of Carbon for Cathode Catalyst Support*, ECS Transactions, **2015**, pp. 1065-1074.